

Honey bee (*Apis mellifera*) hive placement is more influential than orchard layout on the fruit set of a dioecious crop

Jing Li ^{a,*}, Melissa Broussard ^b, Nathan Tomer ^b, Mateusz Jochym ^b, Dilini Fonseka ^{c,d}, Angela Peace ^c, Linley Jesson ^e, Nilsa A. Bosque-Pérez ^f, David Crowder ^g, Brad G. Howlett ^h, David Pattimore ^{b,i}

^a Department of Mathematics, California State University, Northridge, CA, USA

^b The New Zealand Institute for Plant and Food Research Limited, Hamilton, New Zealand

^c Department of Mathematics and Statistics, Texas Tech University, Lubbock, TX, USA

^d Division of Natural Sciences and Mathematics, Southwestern College, Winfield, KS, USA

^e The New Zealand Institute for Plant and Food Research Limited, Auckland, New Zealand

^f Department of Entomology, Plant Pathology and Nematology, University of Idaho, Moscow, ID, USA

^g Department of Entomology, Washington State University, Pullman, WA, USA

^h The New Zealand Institute for Plant and Food Research Limited, Lincoln, New Zealand

ⁱ School of Biological Sciences, University of Auckland, Auckland, New Zealand

ARTICLE INFO

2020 MSC:
92-10
92B05

Keywords:
Pollination
Mathematical modeling
Delay differential equation
Honey bee
Dioecious crop

ABSTRACT

Managers of insect-pollinated orchards face many decisions that can significantly influence crop yields, including managing pollination through use of beehives or the layout of cultivars in the orchard. Understanding the relative importance and interactions between these multiple decisions through empirical field trials is rarely possible, so modeling approaches can provide valuable insights and generate new hypotheses. Based on kiwifruit (*Actinidia chinensis* var. *deliciosa* (A. Chev.) A. Chev. 'Hayward'), a dioecious fruiting vine, as an exemplar, we used a spatially-explicit system of differential equations on a lattice to explore the effects of overlap of male and female flowers, hive placements within the orchard, and orchard layout on the predicted pollination success. In our model, hive placement and orchard layout influenced the proportion of fruit set in an orchard more strongly than male and female flowering synchrony. Simulations with hives distributed evenly around the orchard had the most fruit set, while hives located at a single point resulted in relatively low fruit set. Our model showed that the effect of hive distribution was more important for fruit production than planting regime. We have demonstrated how such a model can be used to provide key information for orchardists to optimize their yields. Our model predicts that while orchard planting decisions are important, the consideration of hive placement during flowering is likely to have greater influence on final orchard productivity in functionally dioecious crops.

1. Introduction

Insect-mediated pollination, primarily by managed Western honey bee (*Apis mellifera* L.) colonies, is critical for fruit set in many cropping systems globally, but is particularly vital for functionally dioecious systems, where pollen must cross from the pollen donor to the pollen recipient for a successful crop (Klein et al., 2007; Rader et al., 2020). This type of dependence is common in horticultural crops with partial or complete self-incompatibility, hybrid seed production, as well as in systems where male and female flowers are borne on separate plants. Kiwifruit (*Actinidia chinensis*) is a dioecious subtropical liana, and a valuable fruit crop, and growers have to make decisions about the

number and distribution of male and female vines to be planted. For pollination, honey bees colonies are typically deployed at a stocking rate of eight hives per hectare; a service orchardists often pay significant amounts for Goodwin (2012), yet placement of hives in an orchard is largely based on logistical constraints for the beekeeper and orchardist rather than what is optimal for pollination. In systems such as kiwifruit, pollination by managed honey bees is seen as crucial owing to the relative scarcity of wild pollinating species (Garibaldi et al., 2013; Howlett et al., 2017); potential pollination deficits are mitigated by paying for the pollination service from honey bees. It is therefore important for growers to be able to make informed decisions about how

* Corresponding author.

E-mail address: jing.li@csun.edu (J. Li).

<https://doi.org/10.1016/j.ecolmodel.2022.110074>

Received 2 March 2022; Received in revised form 21 June 2022; Accepted 10 July 2022

Available online 30 July 2022

0304-3800/© 2022 The Authors. Published by Elsevier B.V. This is an open access article under the CC BY-NC-ND license (<http://creativecommons.org/licenses/by-nc-nd/4.0/>).

best to use these managed pollinators, and how that interacts with other relevant decisions they make in in their orchards.

Models can be used to help understand pollination systems and support decision-making (Ramos-Jiliberto et al., 2018), especially for multiple interacting factors where empirical field trials at orchard scales would be required and almost impossible to fully replicate. Well-studied systems such as kiwifruit, offer an opportunity to develop models which can be parameterized from the literature, and then subsequently used to inform models in other systems. Different model approaches to pollination have been taken over time including models where pollinators are not specifically taken into account (Lescourret et al., 1998a,b), agent-based models (ABM) (Broussard et al., 2022), and spatially homogeneous pollinator dynamical system approaches (Peace et al., 2020). A number of models addressing internal dynamics of *A. mellifera* populations and their interactions with heterogeneous landscapes also have been developed (cf. Table 1 in Joseph et al. (2020)), but they do not specifically address the relationship between pollination management (hive placement, sex ratios in dioecious crops, orchard layout) and pollination efficiency.

Spatial heterogeneity affects pollinator performance, with studies reporting edge effects (Pisanty and Mandelik, 2015), and that planting regimes influence both insect behavior (Jay and Jay, 1984) and pollination success (Testolin, 1991). Additionally, honey bee hive placement in an orchard can affect pollination success; hives that are positioned in a single corner perform less well than when distributed evenly throughout the orchard (Goodwin, 2012). Given the profound effects that landscape configuration can have on pollinator performance and crop production, it is important to consider how to develop spatially explicit mathematical models of pollination.

Broussard et al. (2022) used an ABM framework incorporating spatially explicit flowering and pollinator dynamics to predict fruitset and total yield in kiwifruit. ABM approaches are simulation models that track individual agents and explore system-level emergent behaviors. Broussard and colleagues tracked individual pollinators as they moved across a dynamic orchard, collecting and depositing pollen (Broussard et al., 2022). While ABMs like this are able to incorporate complex individual-level details, they become computationally expensive and their results can be hard to interpret. Dynamical systems offer an alternative modeling approach, by using aggregate-level perspectives and by defining system-level dynamics into differential equations such as ordinary differential equations (ODEs). While these two modeling approaches can yield different predictions, the results when considered can lead to unique insights. For example, it has been shown that analogous models using ODEs and ABM approaches run in parallel can yield valuable complementary insights into understanding cancer growth (Scholl, 2001) and vector-borne pathogens (Shaw et al., 2019, 2017).

Here, we use a dynamical systems approach (ODEs) to develop a spatially explicit model with dynamic flowering and pollinator behaviors in simulated orchards of realistic size and varying orchard layouts. We expand the spatially homogeneous model developed by Peace et al. (2020) to a spatially explicit system of differential equations arranged on a lattice. Moving the previous system of equations to a lattice structure allows us to better model the heterogeneity inherent in field conditions. Movements of bee foragers in the field have been successfully modeled using Brownian or Lévy movement (Vallaeyts et al., 2017), which produce symmetrical predictions for bee movement about the origin, but these models do not take into account density-dependence. There is good evidence that bees change their foraging behavior at high insect densities through a number of mechanisms including rejection of recently visited flowers (Giurfa and Núñez, 1992) and decreasing visit duration to flowers with low resource availability (Keasar et al., 1996), as well as increased traveling distance after visiting several unrewarding flowers (Harder, 1990; Keasar et al., 1996), which would result in density-dependent dynamics. The real-world results of these dynamics have been recorded in kiwifruit, with fruit set declining as

Table 1
Description of model state variables and parameters.

Flower dynamics	
Variable	Meaning
$m(t)$	Number of open male flowers at time t
$f(t)$	Number of open female flowers at time t
Parameter	Meaning
B_m	Number of male buds
B_f	Number of female buds
t_m	Peak day of male flower opening rate
t_f	Peak day of female flower opening rate
σ_m	Spread of male flowering period
σ_f	Spread of female flowering period
τ_m	Life span of male flowering
τ_f	Life span of female flowering
Pollinator dynamics	
Variable	Meaning
P_{m1}	Pollinators with high pollen loads
P_{m2}	Pollinators with medium pollen loads
P_{m3}	Pollinators with low pollen loads
P_f	Pollinators carrying no pollen
Parameter	Meaning
ρ	Pollinators per 1000 flowers
α	Search rate
β	Handling time
δ	Preference to remain on male flowers
ϵ	Preference to remain on female flowers
p_1	Percent chance to set fruit from a single P_{m1} visit
p_2	Percent chance to set fruit from a single P_{m2} visit
p_3	Percent chance to set fruit from a single P_{m3} visit
D	Pollinators' maximum dispersal rate between cells
H	Half dispersal rate pollinators' density
n	The Hill coefficient (indicator of steepness of density-dependence dispersal rate)

distance from male vines is increased (Testolin, 1991). To simulate the movement of bees in accordance to observations in the literature, we used density-dependent stochastic movement between neighboring cells parameterized by Holling Type-II functions (Holling, 1965, 1966).

Using this ODE lattice model, we explored the relative effects of different orchard layouts (placement of functionally male and female plants; a decision made when the orchard is established and can only be changed by regrafting) and honey bee hive placement configurations (a decision made annually by growers and beekeepers) on predicted pollination success.

2. Material and methods

Using kiwifruit as a model for functionally dioecious crops, we developed and analyzed a mathematical model of pollination dynamics that incorporates key features of plant biology and insect behavior on a 1-hectare orchard. In our previous work (Peace et al., 2020), we built a spatially homogeneous model, where bees could visit either floral sex, with different classes of pollinator corresponding to different loading of viable pollen on the insect body. To build on this model and take into account the spatial heterogeneity of the orchard layout and location of beehives, we first divided the orchard into a lattice of 100 by 100 cells; each cell is one meter by one meter. In each cell we assume all conditions for both flower and pollinator are homogeneous. However, conditions across different cells may vary. We first present the model that we used to model the pollination dynamics in one cell without considering the insect movements, then we extend it to include insect movements among cells, to present the full model over the lattice. Table 1 describes the model state variables and parameters.

2.1. Pollination dynamics in one cell of the lattice

Similarly to the model of Peace et al. (2020), at any given cell, without considering any insect movement across cells yet, the pollination dynamics can be described with a combination of flowering dynamics and pollinator dynamics.

2.1.1. Flowering dynamics

We track the number of male and female flowers that have opened using the following differential equations,

$$\frac{dM}{dt} = \frac{B_m}{\sqrt{2\pi\sigma_m^2}} e^{-\frac{(t-t_m)^2}{2\sigma_m^2}}, \tag{1a}$$

$$\frac{dF}{dt} = \frac{B_f}{\sqrt{2\pi\sigma_f^2}} e^{-\frac{(t-t_f)^2}{2\sigma_f^2}}, \tag{1b}$$

where t_m and t_f are the times when the opening rates are highest and σ_m and σ_f are the variations in these rates of opening. With the assumption that each flower is open only for a fixed amount of time, we can determine the number of currently open male flowers ($m(t)$) and female flowers ($f(t)$) using the following expressions:

$$m(t) = \begin{cases} M(t) - M(t - \tau_m), & \text{if } t > \tau_m, \\ M(t), & \text{elsewhere,} \end{cases} \tag{2a}$$

$$f(t) = \begin{cases} F(t) - F(t - \tau_f), & \text{if } t > \tau_f, \\ F(t), & \text{elsewhere,} \end{cases} \tag{2b}$$

where τ_m and τ_f are the numbers of days that male flowers and female flowers remain open.

2.1.2. Pollinator dynamics

Pollinator dynamics are modeled with differential equations that divide the pollinator population into sub-compartments based on their pollen load. Pollinators can have a high, medium, or low pollen load (denoted as P_{m1} , P_{m2} , and P_{m3} respectively) or be carrying no pollen (denoted as P_f). These four states were chosen to represent zero, and three points along an exponential decay curve seen in the literature (Broussard et al., 2021), in accordance with the base model (Peace et al., 2020).

We assume that pollinators completely load up on pollen with a visit to a male flower and deposit some pollen with a visit to a female flower. Empirical data show that pollen dehisces throughout the morning in kiwifruit, becoming limited in the afternoon (Goodwin, 1987; Hopping, 1990; Oh et al., 2020; Chen et al., 1996). This results in pollen availability being highest between 900 and 1300, broadly overlapping with the period of highest insect activity (Malaboeuf et al., 1995; McKay, 1978; Goodwin, 1987; Macfarlane and Ferguson, 1983). Within this 4-hour window, pollen does not appear to be limiting, but is limiting thereafter (Goodwin, 1987). To account for the biological reality that male pollen availability is abundant but limited (which cannot be captured accurately in the dynamic model), we limit the period of active foraging per day to four hours, approximating the window of abundant pollen availability and bee activity (Goodwin, 1987). Fig. 1 depicts the movement of pollinators between the compartments. Pollinators that have just visited a male flower have a high pollen load P_{m1} . These pollinators can either visit another male flower and remain in compartment P_{m1} , or visit a female flower, deposit some pollen and thus be transferred into compartment P_{m2} . Pollinators in compartment P_{m2} with a medium pollen load can either visit a male flower, acquire more pollen, and be transferred into compartment P_{m1} , or visit a female flower, deposit some pollen, and be transferred into compartment P_{m3} . Similarly, pollinators in compartment P_{m3} with a low pollen load can

either visit a male flower, acquire more pollen, and be transferred into compartment P_{m1} or visit a female flower, deposit all their pollen, and be transferred into compartment P_f . Pollinators in compartment P_f , without any pollen, can either visit a female flower and remain in compartment P_f , or visit a male flower, acquire a full load of pollen, and be transferred into compartment P_{m1} .

We used the same definitions introduced in our previous work (Peace et al., 2020) of the total rate at which the pollinators visit male and female flowers, and floral constancy (honey bees have a preference to visit flowers of the same sex as the one they previously visited McKay, 1978; Howpage, 1999; Jay and Jay, 1984; Goodwin and Steven, 1993; Peace et al., 2020). The number of pollinators in each compartment can be tracked using the following system of differential equations:

$$\frac{dP_{m1}}{dt} = \underbrace{\left(\frac{\alpha(f+m)}{1+\alpha\beta(f+m)} \right)}_{\text{Total visitation rate}} \times \left[\underbrace{\left(1 - \left(\frac{f}{f+m} \right)^\epsilon \right)}_{\text{moves from female to male}} (P_{m2} + P_{m3} + P_f) - \underbrace{\left(1 - \left(\frac{m}{f+m} \right)^\delta \right)}_{\text{moves from male to female}} P_{m1} \right], \tag{3a}$$

$$\frac{dP_{m2}}{dt} = \underbrace{\left(\frac{\alpha(f+m)}{1+\alpha\beta(f+m)} \right)}_{\text{Total visitation rate}} \times \left[\underbrace{\left(1 - \left(\frac{m}{f+m} \right)^\delta \right)}_{\text{moves from male to female}} P_{m1} - \underbrace{\left(1 - \left(\frac{f}{f+m} \right)^\epsilon \right)}_{\text{moves from female to male}} P_{m2} - \underbrace{\left(\frac{f}{f+m} \right)^\epsilon}_{\text{moves from female to female}} P_{m2} \right], \tag{3b}$$

$$\frac{dP_{m3}}{dt} = \underbrace{\left(\frac{\alpha(f+m)}{1+\alpha\beta(f+m)} \right)}_{\text{Total visitation rate}} \times \left[\underbrace{\left(\frac{f}{f+m} \right)^\epsilon}_{\text{moves from female to female}} P_{m2} - \underbrace{\left(1 - \left(\frac{f}{f+m} \right)^\epsilon \right)}_{\text{moves from female to male}} P_{m3} - \underbrace{\left(\frac{f}{f+m} \right)^\epsilon}_{\text{moves from female to female}} P_{m3} \right], \tag{3c}$$

$$\frac{dP_f}{dt} = \underbrace{\left(\frac{\alpha(f+m)}{1+\alpha\beta(f+m)} \right)}_{\text{Total visitation rate}} \left[\underbrace{\left(\frac{f}{f+m} \right)^\epsilon}_{\text{moves from female to female}} P_{m3} - \underbrace{\left(1 - \left(\frac{f}{f+m} \right)^\epsilon \right)}_{\text{moves from female to male}} P_f \right], \tag{3d}$$

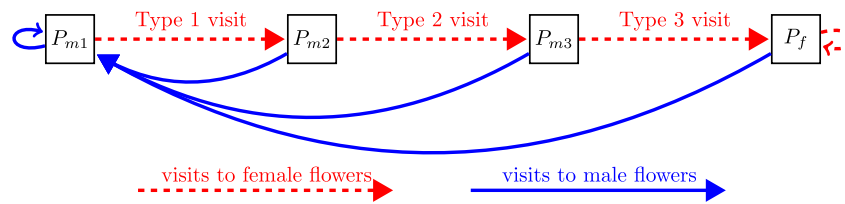


Fig. 1. Structure and flow diagram of bee pollinator compartments inside a cell of the lattice model. Solid blue lines depict visits to a female kiwifruit flower. Dashed red lines depict visits to a male flower.

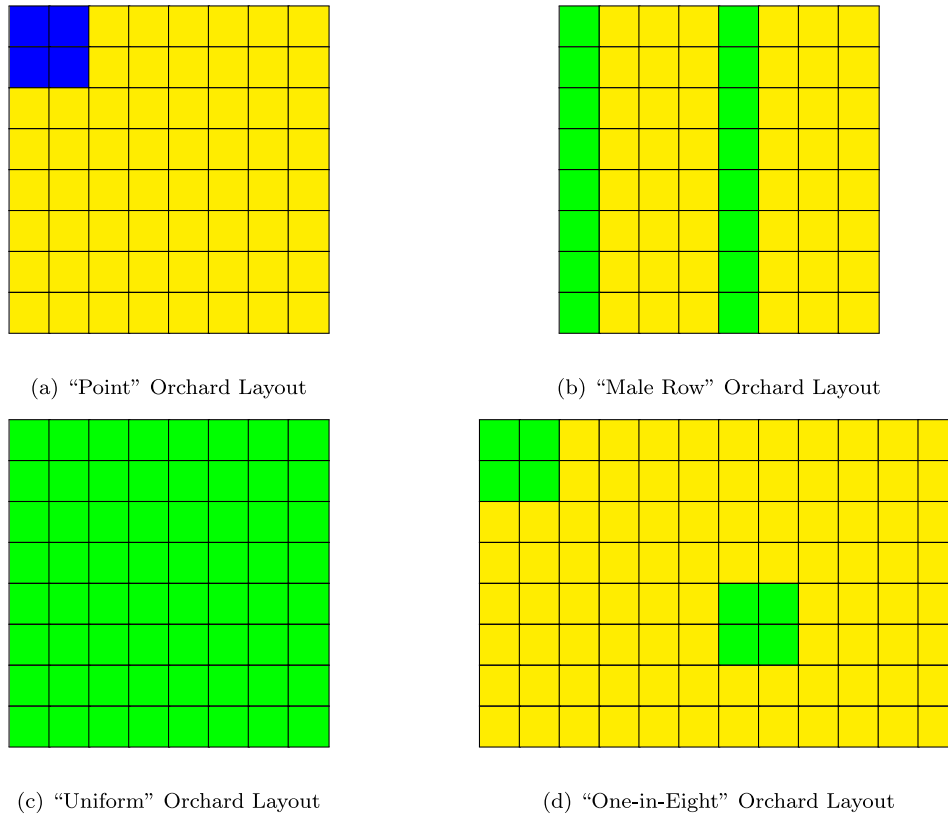


Fig. 2. An illustration of four types of kiwifruit orchards discussed in the model, with blue cells comprised solely of male plants, yellow cells comprised solely of female plants, and green cells with a 50:50 mix of male and female. The subfigures (a)-(c) only use only 8 by 8 cells as examples here. The subfigure (d) uses 8 by 12 cells as an example. For the 1-ha lattice of 100 by 100 cells, the remaining cells in the “Point” orchard layout (a), are all occupied by female flowers. However, the remaining cells in the “Male Row”, “Uniform”, and “One-in-Eight” orchard layouts are repetitions of the illustrated subsets here.

where α is the search rate, β is the handling time, δ and ϵ are the pollinator’s preference to remain on male and female flowers respectively. The incorporation of Eqs. (2) into the system of differential equations for the pollinator model (3) results in a system of ordinary differential equations when $t \leq \min\{\tau_m, \tau_f\}$, before any open flowers begin to close, followed by a system of delayed differential equations with a single delay $\tau = \min\{\tau_m, \tau_f\}$ when $\min\{\tau_m, \tau_f\} \leq t \leq \max\{\tau_m, \tau_f\}$, and then by a system of delayed differential equations with two fixed delays, τ_m and τ_f . This model tracks the number of open male and female flowers (m, f) and the number of pollinators of each type ($P_{m1}, P_{m2}, P_{m3}, P_f$) as they visit male and female flowers in one cell, when the pollinators’ movements between cells are not yet considered.

2.2. The full model: extension to the lattice

To fully capture the pollination dynamics within the entire orchard, we then extended the flower and pollinator dynamics from one cell to the lattice that models the entire orchard. First we denote each cell with (i, j) which is located at the i th row and j th column of the lattice. In our study, we compared four different orchard layouts: “Point”, “Male

Row”, “Uniform”, and “One-in-Eight” (see Fig. 2). We also studied eight possible bee hive arrangements around the orchard (see Fig. 3).

To model the movements of the pollinators from cell to cell in the lattice, we assume that

1. The probability of a pollinator moving out of a cell is density dependent (which is modeled by a Hill function.).
2. After leaving the previously occupied cell, the pollinator will randomly land in one of the 8 neighboring cells (or 5 or 3 if an edge or a corner, respectively).
3. After landing inside a new cell, the pollinator will then visit flowers based on their preference for male flowers (M) or female flowers (F).
4. All bees will return to their hives at the end of each day and there is no carry-over of pollen from day to day.

Let $T^{(i,j)}$ denote the total number flower at cell (i, j) at a given time t ,

$$T^{(i,j)} = f^{(i,j)} + m^{(i,j)}. \tag{4}$$

and denote $P^{(i,j)}$ the total number pollinator at cell (i, j) at a given time t ,

$$P^{(i,j)} = P_{m1}^{(i,j)} + P_{m2}^{(i,j)} + P_{m3}^{(i,j)} + P_f^{(i,j)}. \tag{5}$$

For an interior cell (i, j) , the population dynamics of the pollinators are governed by the following system of impulsive differential equations, during each day, for $t \neq nT$ where T is the length of active foraging period in hours per day.

$$\frac{dP_{m1}^{(i,j)}}{dt} = \underbrace{\left(\frac{\alpha T^{(i,j)}}{1 + \alpha \beta T^{(i,j)}} \right)}_{\text{Total visitation rate}} \left[\underbrace{\left(1 - \left(\frac{f^{(i,j)}}{T^{(i,j)}} \right)^\epsilon \right)}_{\text{moves from female to male}} \left(P_{m2}^{(i,j)} + P_{m3}^{(i,j)} + P_f^{(i,j)} \right) - \underbrace{\left(1 - \left(\frac{m^{(i,j)}}{T^{(i,j)}} \right)^\delta \right)}_{\text{moves from male to female}} P_{m1}^{(i,j)} \right] - 2D \underbrace{\frac{A_{(i,j)} \left(\frac{p^{(i,j)}}{T^{(i,j)}} \right)^n}{H^n + \left(\frac{p^{(i,j)}}{T^{(i,j)}} \right)^n} P_{m1}^{(i,j)} + \sum_{l=i-1}^{i+1} \sum_{k=j-1}^{j+1} D \frac{A_{(l,k)} \left(\frac{p^{(l,k)}}{T^{(l,k)}} \right)^n}{H^n + \left(\frac{p^{(l,k)}}{T^{(l,k)}} \right)^n} P_{m1}^{(l,k)}}_{\text{movements between adjacent cells}}, \tag{6a}$$

$$\frac{dP_{m2}^{(i,j)}}{dt} = \underbrace{\left(\frac{\alpha T^{(i,j)}}{1 + \alpha \beta T^{(i,j)}} \right)}_{\text{Total visitation rate}} \left[\underbrace{\left(1 - \left(\frac{m^{(i,j)}}{T^{(i,j)}} \right)^\delta \right)}_{\text{moves from male to female}} P_{m1}^{(i,j)} - \underbrace{\left(1 - \left(\frac{f^{(i,j)}}{T^{(i,j)}} \right)^\epsilon \right)}_{\text{moves from female to male}} P_{m2}^{(i,j)} - \underbrace{\left(\frac{f^{(i,j)}}{T^{(i,j)}} \right)^\epsilon}_{\text{moves from female to female}} P_{m2}^{(i,j)} \right] - 2D \underbrace{\frac{A_{(i,j)} \left(\frac{p^{(i,j)}}{T^{(i,j)}} \right)^n}{H^n + \left(\frac{p^{(i,j)}}{T^{(i,j)}} \right)^n} P_{m2}^{(i,j)} + \sum_{l=i-1}^{i+1} \sum_{k=j-1}^{j+1} D \frac{A_{(l,k)} \left(\frac{p^{(l,k)}}{T^{(l,k)}} \right)^n}{H^n + \left(\frac{p^{(l,k)}}{T^{(l,k)}} \right)^n} P_{m2}^{(l,k)}}_{\text{movements between adjacent cells}}, \tag{6b}$$

$$\frac{dP_{m3}^{(i,j)}}{dt} = \underbrace{\left(\frac{\alpha T^{(i,j)}}{1 + \alpha \beta T^{(i,j)}} \right)}_{\text{Total visitation rate}} \left[\underbrace{\left(\frac{f^{(i,j)}}{T^{(i,j)}} \right)^\epsilon}_{\text{moves from female to female}} P_{m2}^{(i,j)} - \underbrace{\left(1 - \left(\frac{f^{(i,j)}}{T^{(i,j)}} \right)^\epsilon \right)}_{\text{moves from female to male}} P_{m3}^{(i,j)} - \underbrace{\left(\frac{f^{(i,j)}}{T^{(i,j)}} \right)^\epsilon}_{\text{moves from female to female}} P_{m3}^{(i,j)} \right] - 2D \underbrace{\frac{A_{(i,j)} \left(\frac{p^{(i,j)}}{T^{(i,j)}} \right)^n}{H^n + \left(\frac{p^{(i,j)}}{T^{(i,j)}} \right)^n} P_{m3}^{(i,j)} + \sum_{l=i-1}^{i+1} \sum_{k=j-1}^{j+1} D \frac{A_{(l,k)} \left(\frac{p^{(l,k)}}{T^{(l,k)}} \right)^n}{H^n + \left(\frac{p^{(l,k)}}{T^{(l,k)}} \right)^n} P_{m3}^{(l,k)}}_{\text{movements between adjacent cells}}, \tag{6c}$$

$$\frac{dP_f^{(i,j)}}{dt} = \underbrace{\left(\frac{\alpha T^{(i,j)}}{1 + \alpha \beta T^{(i,j)}} \right)}_{\text{Total visitation rate}} \left[\underbrace{\left(\frac{f^{(i,j)}}{T^{(i,j)}} \right)^\epsilon}_{\text{moves from female to female}} P_{m3}^{(i,j)} - \underbrace{\left(1 - \left(\frac{f^{(i,j)}}{T^{(i,j)}} \right)^\epsilon \right)}_{\text{moves from female to male}} P_f^{(i,j)} \right] \tag{6d}$$

$$-2D \underbrace{\frac{A_{(i,j)} \left(\frac{p^{(i,j)}}{T^{(i,j)}} \right)^n}{H^n + \left(\frac{p^{(i,j)}}{T^{(i,j)}} \right)^n} P_f^{(i,j)} + \sum_{l=i-1}^{i+1} \sum_{k=j-1}^{j+1} D \frac{A_{(l,k)} \left(\frac{p^{(l,k)}}{T^{(l,k)}} \right)^n}{H^n + \left(\frac{p^{(l,k)}}{T^{(l,k)}} \right)^n} P_f^{(l,k)}}_{\text{movements between adjacent cells}}.$$

For the cells in the edge, we have the population dynamics of the pollinators will be governed by a similar system to that in Eq. (6), except the double sum will be replaced with the followings: $\sum_{l=W}^E \sum_{k=S}^N$ =

- $W = i, E = i + 1, S = j - 1, N = j + 1$, for a cell (not at corner) on the left (west side) edge (i, j) ,
- $W = i - 1, E = i, S = j - 1, N = j + 1$, for a cell (not at corner) on the right (east side) edge (i, j) ,
- $W = i - 1, E = i + 1, S = j - 1, N = j$, for a cell (not at corner) on the top (north side) edge (i, j) ,
- $W = i - 1, E = i + 1, S = j, N = j + 1$, for a cell (not at corner) on the bottom (south side) edge (i, j) ,
- $W = i, E = i + 1, S = j - 1, N = j$, for the cell on the top left corner (i, j) ,
- $W = i - 1, E = i, S = j - 1, N = j$, for the cell on the top right corner (i, j) ,
- $W = i, E = i + 1, S = j, N = j + 1$, for the cell on the lower left corner (i, j) ,
- $W = i - 1, E = i, S = j, N = j + 1$, for the cell on the lower right corner (i, j) .

$A_{(i,j)}$ is the adjacent matrix which records the relative probabilities of the pollinators at a given cell moving to one of the neighboring cells. More Specifically,

$$A_{(i,j)} = \begin{cases} \frac{1}{8}, & \text{for an interior cell } (i, j) \text{ which has 8 neighboring cells,} \\ \frac{1}{5}, & \text{for a boundary not a corner cell } (i, j) \text{ which has 5 neighboring cells,} \\ \frac{1}{3}, & \text{for a corner cell } (i, j) \text{ which has 3 neighboring cells.} \end{cases}$$

Under our fourth assumption, when a new day starts, all pollinators will return to the orchard without carrying any pollen. Therefore, at the beginning of each active period of any given day, we assume all pollinators start with P_f . Thus we have when $t = nT$,

$$P_{m1}^{(i,j)}(t) = 0, P_{m2}^{(i,j)}(t) = 0, P_{m3}^{(i,j)}(t) = 0, P_f^{(i,j)}(t) = P_{f0}, \tag{7}$$

where P_{f0} is the total number of pollinators with initial start status at P_f .

At each cell, the flower dynamics is still governed by the following delayed differential equation system

$$f^{(i,j)}(t) = \begin{cases} F^{(i,j)}(t) - F^{(i,j)}(t - \tau_f), & \text{if } t > \tau_f, \\ F^{(i,j)}(t), & \text{elsewhere,} \end{cases}$$

$$m^{(i,j)}(t) = \begin{cases} M^{(i,j)}(t) - M^{(i,j)}(t - \tau_m), & \text{if } t > \tau_m, \\ M^{(i,j)}(t), & \text{elsewhere,} \end{cases}$$

$$\frac{dF^{(i,j)}}{dt} = O_f e^{-\frac{(t - \tau_f)^2}{2\sigma_f^2}}; \quad O_f = \theta_f B_f^{(i,j)}, \tag{8}$$

$$\frac{dM^{(i,j)}}{dt} = O_m e^{-\frac{(t - \tau_m)^2}{2\sigma_m^2}}; \quad O_m = \theta_m B_m^{(i,j)}, \tag{9}$$

where $F^{(i,j)}(t)$ and $M^{(i,j)}(t)$ are the numbers of flowers that have opened up to time t at cell (i, j) . Whereas $f^{(i,j)}(t)$ and $m^{(i,j)}(t)$ are the total number of opened flowers at a given time t at cell (i, j) . $B_m = \sum_{i,j} B_m^{(i,j)}$ and $B_f = \sum_{i,j} B_f^{(i,j)}$ are the total number of male and female buds (flowers) in a given season.

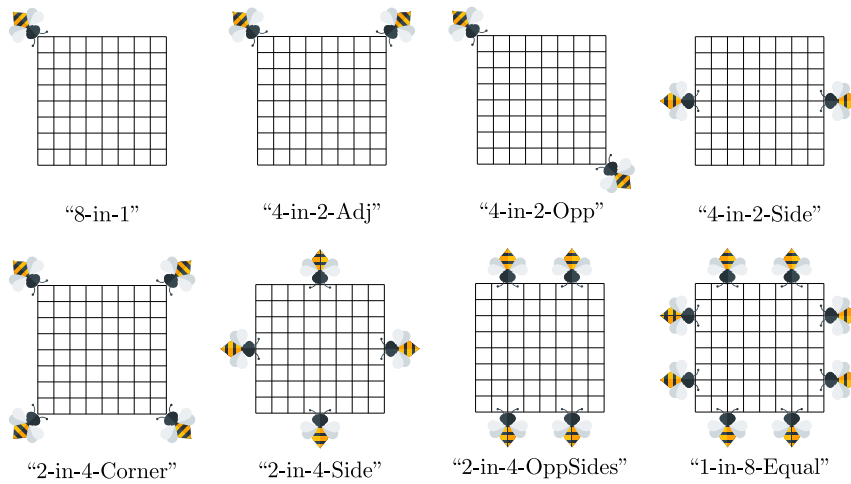


Fig. 3. The range of bee hive placement arrangements compared in a model of pollination dynamics. The full 100 by 100 cell-sized lattice for the kiwifruit orchard is represented here using simplified 8 by 8 cell diagrams, and each bee indicates a location for a beehive(s). In “8-in-1”, all eight beehives are placed in a single location. In “4-in-2-Adj”, “4-in-2-Opp”, and “4-in-2-Side”, four beehives are placed in each location indicated by a bee. In “2-in-4-Corner”, “2-in-4-Side”, and “2-in-4-OppSides”, two beehives are placed in each location indicated by a bee. In “1-in-8-Equal”, one bee hive is placed in each location indicated by a bee.

2.3. Measuring pollination

At each cell, we define the visit that results in transitioning a pollinator from group P_{m1} to P_{m2} as a type one visit, the visit that results in transitioning a pollinator from group P_{m2} to P_{m3} as a type two visit, and the visit that results in transitioning a pollinator from group P_{m3} to P_f as a type three visit (see Fig. 1). We then define fruit set at cell (i, j) for a day t denoted by $Y^{(i,j)}(t)$ as

$$Y^{(i,j)}(t) = 1 - (1 - p_1)^{v_1^{(i,j)}(t)} \times (1 - p_2)^{v_2^{(i,j)}(t)} \times (1 - p_3)^{v_3^{(i,j)}(t)}, \quad (10)$$

where $v_n^{(i,j)}(t)$ for $n = 1, 2, 3$ represents the total number of type n visits that each flower has received at the time of closing (day t), and p_n represents the percentage chance that a single visit will fully pollinate a flower to set fruit, for each visit type n . The total predicted yield at cell (i, j) , denoted $Y_T^{(i,j)}$, is the fruit set for each day multiplied by the number of female flowers closing on that day, summed over all the days,

$$Y_T^{(i,j)} = \sum_t DFC^{(i,j)}(t) * Y^{(i,j)}(t), \quad (11)$$

where $DFC^{(i,j)}(t)$ denotes the daily number of female flowers closing at day t in cell (i, j) . The total predicted yield proportion over all days at cell (i, j) , denoted $Y_P^{(i,j)}$, is the number of flowers closing on each day multiplied by the fruit set for that day divided by the total number of female flowers. In our calculation we use the number of total female flower buds,

$$Y_P^{(i,j)} = \frac{\sum_t DFC^{(i,j)}(t) * Y^{(i,j)}(t)}{B_f^{(i,j)}}. \quad (12)$$

Thus, the overall total predicted yield in the orchard, denoted Y_T , is

$$Y_T = \sum_{i,j} \sum_t DFC^{(i,j)}(t) * Y^{(i,j)}(t), \quad (13)$$

and the overall total predicted yield proportion in the orchard, denoted Y_P , is

$$Y_P = \frac{\sum_{i,j} \sum_t DFC^{(i,j)}(t) * Y^{(i,j)}(t)}{\sum_{i,j} B_f^{(i,j)}}. \quad (14)$$

2.4. Parameterization

All model parameters are listed in Table 2. Most parameters were already parameterized in our previous model, with a sensitivity analysis conducted for them (Peace et al., 2020). We have three new parameters in the extended model, D , H , n , whose values are assumed as there was insufficient empirical data to estimate them. The range of dispersal values (D) were parameterized by using the maximum flight speed of honey bees (30 km/h) (Wenner, 1963) to inform the upper bounds and the value which would result in bees reaching the edge of the 1-ha orchard within the 4-hour foraging period to inform the lower bound. The default value was chosen as the value that resulted in which bees reached the edge of the 1-ha orchard within a 30-minute foraging bout. The range of the half-dispersal rate pollinator’s density, which is defined as the pollinator per thousand flowers density at which the pollinator reaches its half of the maximal dispersal rate, is assumed to be one bee per 1000 flowers to 1000 bees per 1000 flowers (encompassing the range of pollinator densities observed in the field plus one order of magnitude) (Goodwin, 1987). The baseline value is 10 bees per 1000 flowers, a density commonly encountered, and above the value required for adequate pollination, meaning there is likely to be resource competition. The Hill coefficient which indicates the steepness of density-dependence dispersal rate is included for generality, and we choose $n = 1$ for simplicity, owing to lack of sufficient data to support an alternative.

In our previous work (Peace et al., 2020), on the spatially homogeneous base model we conducted a global parameter sensitivity analysis using Latin Hypercube Sampling with the statistical Partial Rank Correlation Coefficient technique to investigate parameter uncertainty. While this parameter sensitivity analysis did not include the three new parameters (D , H , and n), it provides insight for all other parameters. In particular, it showed that the percentage of female flowers $B_f / (B_m + B_f)$, the total number of buds $(B_m + B_f)$, and the bee density (ρ) have the most significant positive effect on the total predicted yield. The pollinators’ preference to remain on female flowers (ϵ), the male flowering period (σ_m), and the pollinator’s preference to remain on male flowers (δ) are the next most important parameters increasing the predicted yield. Furthermore, pollinator handling time (β) is the only parameter with a strongly negative effect on the total predicted yield. For this extended model we explore various ranges of D and H in Appendix.

Table 2

Model parameters, base values and ranges used in simulations. Parameters were parameterized by Peace et al. (2020), except the new parameters D , H , n .

Parameter	Meaning	Units	Base value	Range	References
α	Search rate	1/(day \times flower)	480	120–3600	Broussard et al. (2022)
β	Handling time	Days	0.0011	0.00013–0.0094	McKay (1978), Macfarlane and Ferguson (1983), Vaissière et al. (1996) and Goodwin et al. (2013)
δ	Preference to remain on male flower	–	0.0634	0–1	McKay (1978), Jay and Jay (1984), Goodwin and Steven (1993), Howpage (1999) and Broussard et al. (2022)
ϵ	Preference to remain on female flower	–	0.0725	0–1	McKay (1978) and Broussard et al. (2022)
B_m	Number of male buds	Flower	600 000	300 000–900 000	Brundell (1975) and Testolin (1991)
B_f	Number of female buds	Flower	600 000	300 000–900 000	Brundell (1975)
t_m	Peak day of male flower opening	Day	6	2–9	Brundell (1975), Costa et al. (1993), Howpage (1999) and Gonzalez et al. (1994)
t_f	Peak day of female flower opening	Day	6	2–9	Brundell (1975), Costa et al. (1993), Howpage (1999) and Gonzalez et al. (1994)
σ_m	Spread of male flowering period	–	2.5	0.5–5.5	Brundell (1975), Howpage (1999) and Gonzalez et al. (1994)
σ_f	Spread of female flowering period	–	2	1–4	Brundell (1975), Howpage (1999) and Gonzalez et al. (1994)
τ_m	Life span of male flowering	Day	4	3–5	Goodwin (1987)
τ_f	Life span of female flower	Day	5	3–7	Hopping (1990), Goodwin and Steven (1993) and González et al. (1995)
ρ	Pollinators per 1000 flowers	Pollinators/1000 flowers	6	1–20	Goodwin (1987) and Testolin (1991)
p_1	Percent chance to set fruit from single type one visit	–	0.66	0.25–0.75	Broussard et al. (2022)
p_2	Percent chance to set fruit from single type two visit	–	0.55	0.1–0.65	Broussard et al. (2022)
p_3	Percent chance to set fruit from single type three visit	–	0.22	0–0.5	Broussard et al. (2022)
D	Pollinators' maximum dispersal rate between cells	Per time	1500	500–2500	Assumed
H	Half dispersal rate pollinators' density	Pollinators/1000 flowers	10	1–1000	Assumed
n	The Hill coefficient (indicator of steepness of density-dependence dispersal rate)	–	1	–	Assumed

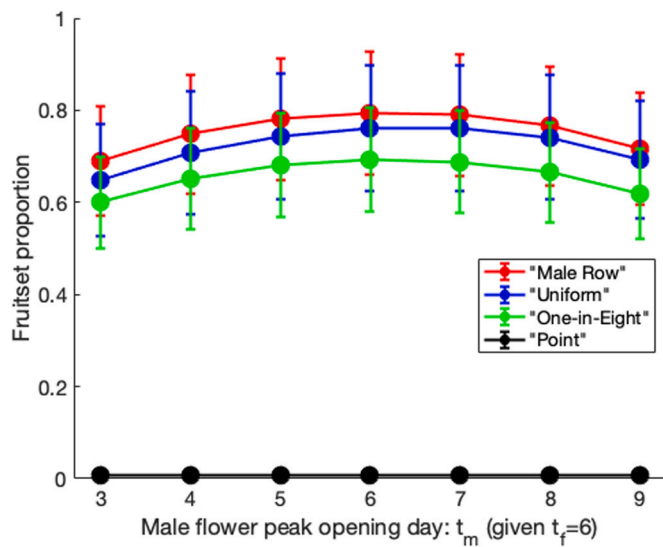


Fig. 4. Proportion of fruit set in simulated kiwifruit orchards with differing planting regimes and bloom synchronies, under the assumption that the peak opening day of female flowers is on day six. Dots represent the average fruit set across all eight bee hive placements, and bars represent the range. The total number of male and female flowers was identical across the four scenarios.

2.5. Model simulations

We programmed the simulations in Matlab (MATLAB) using differential equation solvers ode45 with initial conditions such that 0% of pollinators were P_{m1} , P_{m2} , and P_{m3} , and 100% of pollinators were P_f at

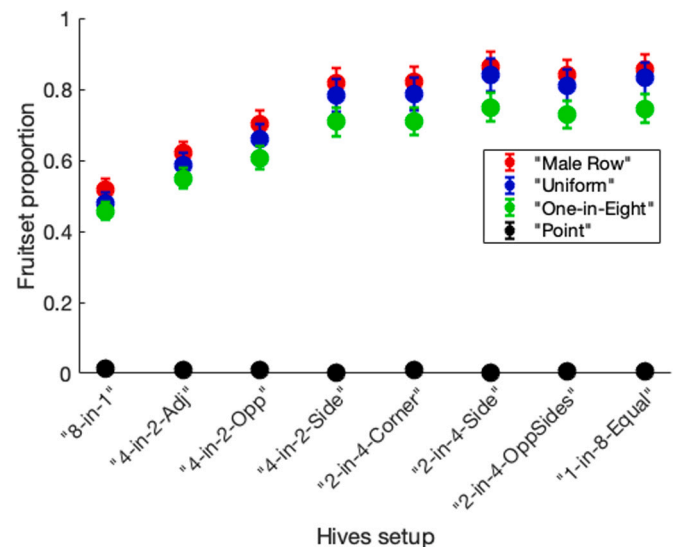


Fig. 5. Proportion of fruit set in simulated kiwifruit orchards with differing planting regimes and bee hive placements. Dots represent the average performance of each orchard layout at each hive placement configuration across a range of bloom synchrony values, while bars represent the range. The total number of male and female flowers was identical across the four scenarios.

time $t = 0$ for an orchard of sample of one ha in size. Parameter values for the total number of flower buds B_m (male) and B_f (female) along with the number of pollinators per 1000 female flowers ρ were used to determine the total number of pollinators for each simulation. The simulations were performed in a high performance computing cluster

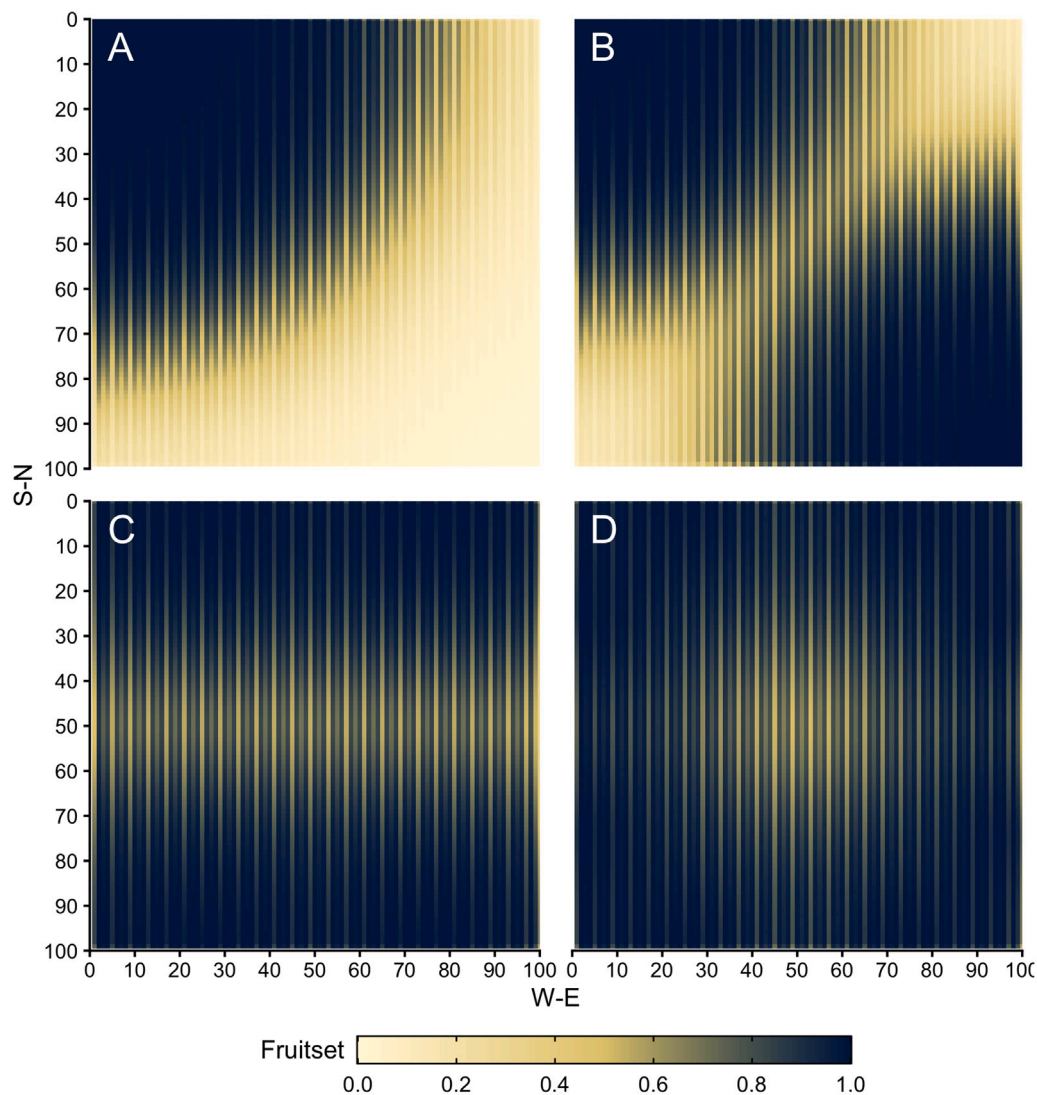


Fig. 6. Heatmaps for the predicted fruit set on a 1-ha “Male Row” kiwifruit orchard with four different bee hive placements. A: “8-in-1”; B: “4-in-2-Opp”; C: “2-in-4-OppSides”; D: “1-in-8-Equal”. The total number of male and female flowers was identical across all hive placement scenarios.

based on CentOS Linux 7, with OpenLava 3.2.0 load scheduling facility; simulation runs were parallelized with a custom script written in R (R Core Team, 2020) using the *foreach* package (Microsoft and Weston, 2020).

3. Results

Like Peace et al. (2020), our model predicted that fruit set decreased with decreasing overlap of male and female kiwifruit cultivars. In addition, we found that different orchard layouts affected fruit set alongside synchrony, with the commonly-used “Male Row” layout outperforming all other layouts (Fig. 4). For the three layouts that would potentially be used by orchardists (excluding the extreme layout “Point”), the variation in fruit set between layouts was smaller than the variation in fruit set between different hive placement regimes.

Overall, the effect of synchrony was less than the effects of both hive setup and orchard layout (Fig. 5), although our values were constrained to a possible mismatch of only three days. With less synchrony, the potential for fruit set decreases further, but in these extreme scenarios better pollination is unlikely to make up for the lack of synchrony.

Placing all hives in a single location resulted in the lowest fruit set across all three field-realistic orchards, while distributing hives evenly around the orchard resulted in the highest fruit set. Of the intermediary

designs, breaking hives into four clusters performed nearly as well as eight, and placing two groups of hives, one on either side of the orchard, performed nearly as well. The combination of pulsing and diffusion resulted in each hive effectively pollinating a limited radius from its placement location; the extend of white shown in the figures displaying the spatial pattern of fruit set indicates areas with very low fruit set (Fig. 6). The 4-in-2-Opp and 8-in-1 and layouts resulted in negligible fruit set across approximately 1/6 and 1/3 and of the orchards respectively (roughly equivalent to a 15%–30% decline in yield).

4. Discussion

We found that there were effects of both orchard type and hive placement on predicted pollination success. For the unrealistic “Point” layout, where all male flowers occur in a small corner of the simulated 1-ha orchard, changing the location of hives was unable to bring yield up to economical levels. For the typical orchard configurations encountered in kiwifruit (*i.e.*, excluding “Point”), hive placement had a larger effect than planting regime. This finding is potentially good news for orchardists, as it is much more straightforward to change where hives are placed in an orchard than to change the existing planting arrangement. The latter requires a considerable investment of both time

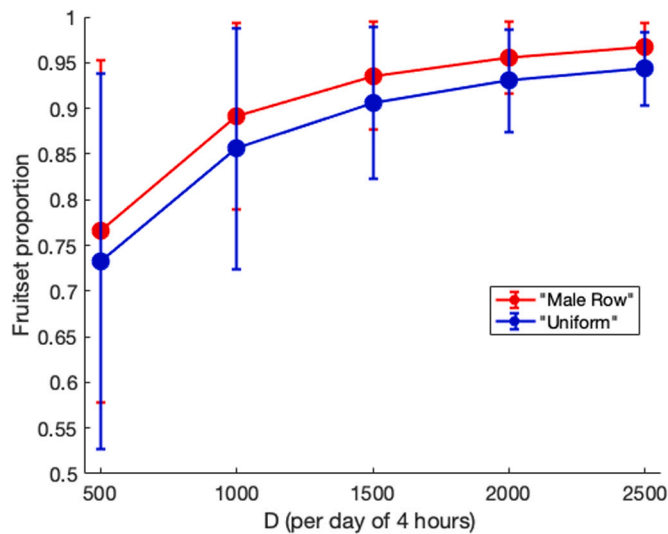


Fig. 7. Proportion of fruit set in simulated kiwifruit orchards with differing planting regime, hive placements, and a bee’s maximum dispersal rate ranging from 500 to 2500. Dots represent the average fruit set across all eight hive placements, and bars represent the range of eight hive placements.

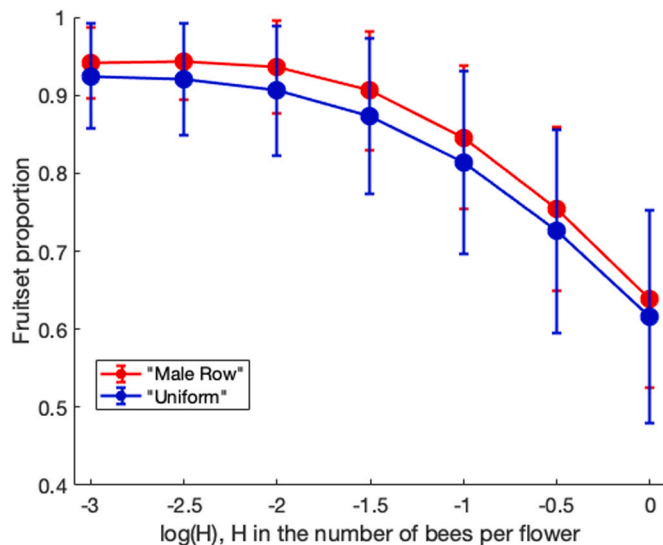


Fig. 8. Proportion of fruit set in simulated kiwifruit orchards with differing planting regime (“Male Row” and “Uniform”), eight bee hive placements, and half dispersal rate pollinator’s density ranging from 0.001 to 1 (plotted in Log scale). Dots represent the average fruit set across all eight hive placements, and bars represent the range of eight hive placements.

and money (both direct expense and loss of income) while plants are grafted and growing.

The hive placements we examined were focused on delivering hives to the perimeter of the orchard as, while it may be recommended to distribute hives throughout the orchard for best results (Goodwin, 2012), growers and beekeepers are often constrained by logistics and capacity to this time-consuming task at a critically busy time of year. We examined the effects of deploying the recommended eight hives/ha in eight different of placements at either one, two, four, or eight sites surrounding the orchard. Of note is that several placements produced very similar results to the theoretical best placement (“1-in-8-Equal”–hives at 8 locations around the orchard). All the options for four hive drop sites (“2-in-4-Corner”, “2-in-4-Side”, “2-in-4-OppSides”) performed similarly to “1-in-8-Equal”, yielding economical returns, as did

“4-in-2-Side”, where two groups of four hives were dropped on opposite sides of the orchard. This result is of particular importance as it would yield the most pollination success for the least beekeeper effort. Our model has shown significantly utility in being able to predict optimum and near-optimum scenarios that could make a substantial economic benefit for growers.

A possible shortcoming of our approach is that our model results in circular ‘spheres of influence’ for each hive or hive group. In reality, this pattern is likely to be somewhat elliptical, probably because of the preference for bees to work down rows rather than across them (Free, 1966; Boerma and Moradshahi, 1975; Jay and Jay, 1984; Evans et al., 2011). However, in an experiment where male flowers were removed from all but one vine (a setup similar to our ‘point’ orchard), fruit set was arranged approximately circularly around the male vine (Testolin, 1991), indicating that bees are foraging equally in all directions. This being the case, our model suggests that there is a benefit to having hives distributed around the perimeter of the orchard, and that more locations is generally better, but they do not need necessarily to be deployed as single hives to achieve the majority of the benefit.

The similar performance of several of the orchard layouts may be partly due to our model incorporating a rate of diffusion, which led to full coverage of the orchard by bees under most scenarios (see also the discussion in the Appendix). If there are real-world factors that decrease this movement of bees through a 1-ha block, more divergence in fruit set between layouts might be experienced. For example, in crops prone to wind damage, individual blocks can be smaller than 1-ha and separated by large wind-breaks. Other orchards utilize netting between rows which might modify pollinator movement, or have orchards planted in irregular sized blocks that alter the distance pollinators need to travel to reach the entire block. Our model did not account for varying pollinator numbers due to competing bloom outside the orchard, or in fact any wider context for the 1-ha block. The power of this model lies in its ability to generate new hypotheses about optimal pollination scenarios and to consider the relative importance of multiple different factors at once.

Additionally, we found that optimal hive placement can partially compensate for poor bloom synchrony—a key concern not only for kiwifruit growers, but also for producers of functionally dioecious crops more generally. Bloom synchrony in any given season is a combination of the characteristics of the cultivars and their response to the environmental conditions they have experienced, factors which are beyond the control of the orchardist during flowering. In contrast, hive placement (and density Peace et al., 2020) can be rapidly altered in response to observations of conditions, and thus limit losses.

Both ABM and ODE models have provided useful insights into key decisions made by orchardists that potentially have a large economic effect. Incorporating spatial-positioning information is particularly valuable because of the importance of space and time in pollination. Intuitively we found that hive placement in the orchard has a very large influence on fruit production, which is fortunate as it is an easily managed variable (compared with plantings of long-lived perennial plants). It is likely that future models will be able to incorporate more realistic foraging by pollinators using this template, and will be able to reveal further insights into methods to optimize pollination.

CRedit authorship contribution statement

Jing Li: Conceptualization, Methodology, Formal analysis, Writing – original draft, Writing – review & editing. **Melissa Broussard:** Conceptualization, Methodology, Formal analysis, Writing – original draft, Writing – review & editing. **Nathan Tomer:** Conceptualization, Methodology, Formal analysis, Writing – original draft, Writing – review & editing. **Mateusz Jochym:** Conceptualization, Methodology, Formal analysis, Writing – original draft, Writing – review & editing. **Dilini Fonseka:** Conceptualization, Formal analysis, Writing – original draft,

Writing – review & editing. **Angela Peace:** Conceptualization, Methodology, Formal analysis, Writing – original draft, Writing – review & editing. **Linley Jesson:** Conceptualization, Writing – original draft, Writing – review & editing. **Nilsa A. Bosque-Pérez:** Conceptualization, Writing – original draft, Writing – review & editing. **David Crowder:** Conceptualization, Writing – original draft, Writing – review & editing. **Brad G. Howlett:** Conceptualization, Writing – original draft, Writing – review & editing. **David Pattemore:** Conceptualization, Methodology, Supervision, Writing – original draft, Writing – review & editing.

Declaration of competing interest

The authors declare that they have no known competing financial interests or personal relationships that could have appeared to influence the work reported in this paper.

Data availability

Data will be made available on request.

Acknowledgments

The work was conducted with funding from the Plant & Food Research Discovery Science grant DS 14-65. We would like to thank Mark Goodwin for his assistance in obtaining data for model parameterization, and Allison Shaw for stimulating discussion that contributed to model development.

Appendix

To better support our parameterization on D and H , we also simulated the model system with varying values for D and H respectively. The results of varying D values ranging from 500 to 3000 are presented in Fig. 7. The average proportion of fruit set across eight hives placements increases with the maximal pollinator's dispersal rate. When $D = 1500$, the predicted range for fruit set is above 80% for both "Male Row" and "Uniform". Such prediction confirms our selection of the D value in the model simulation. Fig. 8 presents the results of proportion of fruit set in simulated orchards with differing planting regime ("Male Row" and "Uniform"), eight hive replacements, and half dispersal rate pollinator's density ranging from 0.001 to 1. The average proportion of fruit set across eight hives placements decreases with increasing half dispersal rate pollinator's density. When $H = 0.01$, the predicted range for fruit set is above 80% for both "Male Row" and "Uniform". This prediction supports the choice of the H value in our model simulation in Section 3.

References

Boerma, H., Moradshahi, A., 1975. Pollen movement within and between rows to male-sterile soybeans. *Crop Sci.* 15 (6), 858–861. <http://dx.doi.org/10.2135/CROPSCI1975.0011183X001500060033X>.

Broussard, M.A., Goodwin, M., McBrydie, H.M., Evans, L.J., Pattemore, D.E., 2021. Pollination requirements of kiwifruit (*Actinidia chinensis* Planch.) differ between cultivars 'Hayward' and 'Zesy002'. *N. Z. J. Crop Hortic. Sci.* 49 (1), 30–40. <http://dx.doi.org/10.1080/01140671.2020.1861032>.

Broussard, M., Jochym, M., Tomer, N., Jesson, L., Shaw, A., Crowder, D., Bosque-Pérez, N., Li, J., Peace, A., Fonseka, D., Howlett, B., Pattemore, D., 2022. Using agent-based models to predict pollen deposition in a dioecious crop. in preparation.

Brundell, D., 1975. Flower development of the Chinese gooseberry (*Actinidia chinensis* Planch.) II. Development of the flower bud. *N. Z. J. Bot.* 13 (3), 485–496. <http://dx.doi.org/10.1080/0028825X.1975.10430338>.

Chen, Y., Li, H., Zhu, D., Zhai, Y., 1996. A study on the viability and storage time of the pollen for *Actinidia*. *Acta Agric. Univ. Henanensis* 30 (2), 175–177. <http://europepmc.org/abstract/CBA/293334>.

Costa, G., Testolin, R., Vizzotto, G., 1993. Kiwifruit pollination: an unbiased estimate of wind and bee contribution. *N. Z. J. Crop Hortic. Sci.* 21 (2), 189–195. <http://dx.doi.org/10.1080/01140671.1993.9513767>.

Evans, L., Goodwin, R., Walker, M., Howlett, B., 2011. Honey bee (*Apis mellifera*) distribution and behaviour on hybrid radish (*Raphanus sativus* L.) crops. *N. Z. Plant Prot.* 64, 32–36. <http://dx.doi.org/10.30843/nzpp.2011.64.5952>.

Free, J., 1966. The foraging areas of honeybees in an orchard of standard apple trees. *J. Appl. Ecol.* 3 (2), 261–268. <http://dx.doi.org/10.2307/2401251>.

Garibaldi, L.A., Steffan-Dewenter, I., Winfree, R., Aizen, M.A., Bommarco, R., Cunningham, S.A., Kremen, C., Carvalheiro, L.G., Harder, L.D., Afik, O., et al., 2013. Wild pollinators enhance fruit set of crops regardless of honey bee abundance. *Science* 339 (6127), 1608–1611.

Giurfa, M., Núñez, J.A., 1992. Honeybees mark with scent and reject recently visited flowers. *Oecologia* 89 (1), 113–117. <http://dx.doi.org/10.1007/BF00319022>.

Gonzalez, M., Coque, M., Herrero, M., 1994. Pollinator selection in kiwifruit (*Actinidia deliciosa*). *J. Hortic. Sci.* 69 (4), 697–702. <http://dx.doi.org/10.1080/14620316.1994.11516502>.

González, M., Coque, M., Herrero, M., 1995. Stigmatic receptivity limits the effective pollination period in kiwifruit. *J. Amer. Soc. Hortic. Sci.* 120, 199–202.

Goodwin, R.M., 1987. Ecology of honey bee (*Apis mellifera* L.) pollination of kiwifruit (*Actinidia deliciosa* A. Chev.) (Ph.D. thesis). University of Auckland.

Goodwin, M., 2012. Pollination of Crops in Australia and New Zealand. Rural Industries Research and Development Corporation, Ruakura, New Zealand.

Goodwin, R., McBrydie, H., Taylor, M., 2013. Wind and honey bee pollination of kiwifruit (*Actinidia chinensis* 'HORT16A'). *N. Z. J. Bot.* 51 (3), 229–240. <http://dx.doi.org/10.1080/0028825X.2013.806934>.

Goodwin, R., Steven, D., 1993. Behaviour of honey bees visiting kiwifruit flowers. *N. Z. J. Crop Hortic. Sci.* 21 (1), 17–24. <http://dx.doi.org/10.1080/01140671.1993.9513741>.

Harder, L.D., 1990. Behavioral responses by bumble bees to variation in pollen availability. *Oecologia* 85 (1), 41–47. <http://dx.doi.org/10.1007/BF00317341>.

Holling, C.S., 1965. The functional response of predators to prey density and its role in mimicry and population regulation. *Mem. Entomol. Soc. Canada* 97 (S45), 5–60. <http://dx.doi.org/10.4039/entm9745fv>.

Holling, C.S., 1966. The functional response of invertebrate predators to prey density. *Mem. Entomol. Soc. Canada* 98 (S48), 5–86. <http://dx.doi.org/10.4039/entm9848fv>.

Hopping, M., 1990. *Floral Biology, Pollination and Fruit Set*. Bennetts Book Centre Ltd, Massey University, pp. 71–96, Ch. Floral biology, pollination and fruit set.

Howlett, B., Read, S., Jesson, L., Benoist, A., Evans, L., Pattemore, D., 2017. Diurnal insect visitation patterns to 'Hayward' kiwifruit flowers in New Zealand. *N. Z. Plant Prot.* 70, 52–57. <http://dx.doi.org/10.30843/nzpp.2017.70.27>.

Howpage, D., 1999. *Pollination Biology of Kiwifruit: Influence of Honey Bees, Apis mellifera* L. (Ph.D. thesis).

Jay, D., Jay, C., 1984. Observations of honeybees on Chinese gooseberries ('kiwifruit') in New Zealand. *Bee World* 65 (4), 155–166. <http://dx.doi.org/10.1080/0005772X.1984.11098804>.

Joseph, J., Santibáñez, F., Laguna, M.F., Abramson, G., Kuperman, M.N., Garibaldi, L.A., 2020. A spatially extended model to assess the role of landscape structure on the pollination service of *Apis mellifera*. *Ecol. Model.* 431, 109201. <http://dx.doi.org/10.1016/j.ecolmodel.2020.109201>.

Keasar, T., Shmida, A., Motro, U., 1996. Innate movement rules in foraging bees: flight distances are affected by recent rewards and are correlated with choice of flower type. *Behav. Ecol. Sociobiol.* 39 (6), 381–388. <http://www.jstor.org/stable/4601282>.

Klein, A.-M., Vaissière, B.E., Cane, J.H., Steffan-Dewenter, I., Cunningham, S.A., Kremen, C., Tscharntke, T., 2007. Importance of pollinators in changing landscapes for world crops. *Proc. R. Soc. B: Biol. Sci.* 274 (1608), 303–313. <http://dx.doi.org/10.1098/rspb.2006.3721>.

Lescourret, F., Génard, M., Habib, R., Pailly, O., 1998a. Pollination and fruit growth models for studying the management of kiwifruit orchards. II. Models behaviour. *Agric. Syst.* 56 (1), 91–123. [http://dx.doi.org/10.1016/S0308-521X\(97\)00043-7](http://dx.doi.org/10.1016/S0308-521X(97)00043-7).

Lescourret, F., Habib, R., Génard, M., Agostini, D., Chadouef, J., 1998b. Pollination and fruit growth models for studying the management of kiwifruit orchards. I. Models description. *Agric. Syst.* 56 (1), 67–89. [http://dx.doi.org/10.1016/S0308-521X\(97\)00042-5](http://dx.doi.org/10.1016/S0308-521X(97)00042-5).

Macfarlane, R., Ferguson, A., 1983. *The 1980 to 1982 Kiwifruit Survey of Pollination Report*, DSIR.

Malabouef, F., Vaissière, B., Cour, P., 1995. Pollen flow in the atmosphere of kiwifruit (*Actinidia deliciosa*) orchards. In: III International Symposium on Kiwifruit, Vol. 444. pp. 413–418. <http://dx.doi.org/10.17660/ActaHortic.1997.444.64>.

MATLAB, version R2019a. The MathWorks Inc. Natick, Massachusetts. <https://www.mathworks.com/>.

McKay, S., 1978. *Pollination and Other Factors Affecting Fruit-Set and Size of Kiwifruit* (Master's thesis). University of California, Davis.

Microsoft, Weston, S., 2020. Foreach: Provides foreach looping construct. R package version 1.5.0. <https://CRAN.R-project.org/package=foreach>.

Oh, E.U., Jeong, S.Y., Kang, H.H., Song, K.J., 2020. Characterization of pollen development in staminate kiwifruit (*Actinidia* sp.) cultivars. pp. 1–8. <http://dx.doi.org/10.7235/HORT.20200001>.

- Peace, A., Pattermore, D., Broussard, M., Fonseca, D., Tomer, N., Bosque-Pérez, N.A., Crowder, D., Shaw, A.K., Jesson, L., Howlett, B.G., Jochym, M., Li, J., 2020. Orchard layout and plant traits influence fruit yield more strongly than pollinator behaviour and density in a dioecious crop. *PLoS One* 15 (10), e0231120. <http://dx.doi.org/10.1371/journal.pone.0231120>.
- Pisanty, G., Mandelik, Y., 2015. Profiling crop pollinators: life history traits predict habitat use and crop visitation by Mediterranean wild bees. *Ecol. Appl.* 25 (3), 742–752. <http://dx.doi.org/10.1890/14-0910.1>.
- R Core Team, 2020. R: A Language and Environment for Statistical Computing. R Foundation for Statistical Computing, Vienna, Austria, R version 4.0.0. <https://www.R-project.org/>.
- Rader, R., Cunningham, S., Howlett, B., Inouye, D., 2020. Non-bee insects as visitors and pollinators of crops: Biology, ecology, and management. *Annu. Rev. Entomol.* 65 (1), 391–407. <http://dx.doi.org/10.1146/annurev-ento-011019-025055>, PMID: 31610136.
- Ramos-Jiliberto, R., de Espanés, P.M., Franco-Cisterna, M., Petanidou, T., Vázquez, D.P., 2018. Phenology determines the robustness of plant–pollinator networks. *Sci. Rep.* 8 (1), 14873. <http://dx.doi.org/10.1038/s41598-018-33265-6>.
- Scholl, H., 2001. Agent-based and system dynamics modeling: A call for cross study and joint research. In: *Proceeding of the 34th Annual Hawaii International Conference on System Sciences*, 2001. IEEE, pp. 1–8. <http://dx.doi.org/10.1109/HICSS.2001.926296>.
- Shaw, A.K., Igoe, M., Power, A.G., Bosque-Pérez, N.A., Peace, A., 2019. Modeling approach influences dynamics of a Vector-Borne pathogen system. *Bull. Math. Biol.* 81, 2011–2028. <http://dx.doi.org/10.1007/s11538-019-00595-z>.
- Shaw, A.K., Peace, A., Power, A.G., Bosque-Pérez, N.A., 2017. Vector population growth and condition-dependent movement drive the spread of plant pathogens. *Ecology* 98 (8), 2145–2157. <http://dx.doi.org/10.1002/ecy.1907>.
- Testolin, R., 1991. Male density and arrangement in kiwifruit orchards. *Sci. Hortic.* 48 (1), 41–50. [http://dx.doi.org/10.1016/0304-4238\(91\)90151-N](http://dx.doi.org/10.1016/0304-4238(91)90151-N).
- Vaissière, B., Rodet, G., Cousin, M., Botella, L., Torrè Grossa, J.-P., 1996. Pollination effectiveness of honey bees (Hymenoptera: Apidae) in a Kiwifruit Orchard. *J. Econ. Entomol.* 89 (2), 453–461. <http://dx.doi.org/10.1093/jee/89.2.453>.
- Vallaëys, V., Tyson, R.C., Lane, W.D., Deleersnijder, E., Hanert, E., 2017. A Lévy-flight diffusion model to predict transgenic pollen dispersal. *J. R. Soc. Interface* 14 (126), 20160889. <http://dx.doi.org/10.1098/rsif.2016.0889>.
- Wenner, A., 1963. The flight speed of honeybees: a quantitative approach. *J. Apicult. Res.* 2 (1), 25–32. <http://dx.doi.org/10.1080/00218839.1963.11100053>.